Supplementary Information (SI) for Nanoscale.
This journal is © The Royal Society of Chemistry 2024

Supplementary Information

Quantitative photocurrent scanning probe microscopy on PbS quantum dot monolayers

Florian Küstner[a], Harald Ditlbacher[a], Andreas Hohenau[a], Dmitry N. Dirin[bc], Makysm Kovalenko[bc], and Joachim R. Krenn[a]

[a]Institute of Physics, University of Graz, 8010 Graz, Austria
[b]Institute of Inorganic Chemistry, Department of Chemistry and Applied Biosciences, ETH Zürich, 8093 Zürich, Switzerland
[c]Empa - Swiss Federal Laboratories for Materials Science and Technology, Laboratory for Thin Films and Photovoltaics, 8600 Dübendorf, Switzerland

S1 Estimation of the local irradiance

For experimental convenience, the laser power P was measured before entering the microscope. From reference measurements it was determined that the laser power P_0 focused on the sample position corresponds to 75% of the power present before entering the microscope. The intensity I_c at the center of the focus of a low N.A. objective is given by

$$I_c = P_0 \frac{\pi r^2}{\lambda^2 f^2} , \tag{S1}$$

with the laser wavelength λ, the illuminated lens radius r and the focal length f [1]. For the 10× objective with N.A.=0.3 and for the used laser wavelength of 633 nm, the intensity at the center of the focus is then given by

$$I_c = 0.75 \cdot P \cdot 70 \cdot 10^6 \text{ cm}^{-2} . \tag{S2}$$

For the 60× oil immersion objective with N.A.=1.4 the intensity at the center of the focus, as retrieved from a numerical simulation is

$$I_c = 0.75 \cdot P \cdot 0.9 \cdot 10^9 \text{ cm}^{-2} . \tag{S3}$$

S2 Estimation of the number of contacted QDs

The AFM tip is assumed to have a spherical shape with radius r. It is further assumed that the tip has a penetration depth Δ into the sample. The radius R of the contact area, as sketched in Fig. S1, is then given as

$$R^2 = 2r\Delta - \Delta^2. \tag{S4}$$

In Tab. S1, the number of contacted QDs (diameter 3.2 nm) in a densely packed monolayer contacted by an AFM tip with a radius r of 25 nm is listed for some reasonable values of Δ.

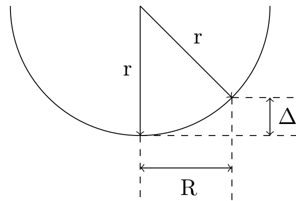

Fig. S1 Sketch of a AFM tip with radius r and penetration depth Δ. R is the radius of the contact area.

Tab. S1 Contact area $A = R^2\pi$ and average number of QDs (diameter 3.2 nm) in a densely packed monolayer, contacted by an AFM tip with radius of 25 nm. Values of Δ = 0.1-1.0 are considered.

Δ / nm	A / nm^2	#QDs
0.1	16	1.7
0.2	31	3.5
0.3	47	5.3
0.5	78	8.8
1.0	154	17.4

S3 I/V model

Several models have been successfully applied to describe I/V curves measured for metal/semiconductor/metal systems. On one hand, the empirical model

$$I(V) = \frac{V}{R_0} \exp\left(\frac{V}{V_0}\right), \tag{S5}$$

was used to determine the parameters known as sheet resistance R_0 and voltage barrier V_0 [2]. However, since we measure asymmetrical I/V curves, this approach seems to be unsuitable. Furthermore, the concept of a sheet resistance can be questioned when it comes to just a few QDs bridging the electrodes[3]. On the other hand, semi-empirical thermionic emission models based on the presence of a Schottky barrier were applied [4]. In these models, the two interfaces and the bulk of the semiconductor are described individually and the resulting system of equations is solved [5,6]. This approach is expected to lose its validity when the semiconductor layer becomes so thin that the depletion layers at the two interfaces begin to overlap. Certainly for a QD monolayer the two interfaces (to the sample and to the AFM tip) cannot be treated independently.

Here, we describe the current flow across an illuminated QD layer by a superposition of a drift current of photo-excited charge carriers in the QDs and a diffusion current across the interface barriers based on a single Schottky barrier model. As theoretically described for semiconductors[7] and experimentally observed for QDs[8], the density of photo-excited charge carriers (and thus the conductivity) follows a power-law with respect to the applied light irradiance P. In our setup we illuminate an area of about $1\,\mu\mathrm{m}^2$ and probe just a few QDs with the pcAFM tip. We therefore assume that a reservoir of excited charge carriers forms around the contacted QDs that also follows a power law which can therefore be probed by the tip. We thus model the photo-excited drift current I_{ph} for an applied external voltage V_{ext} as

$$I_{\mathrm{ph}} = KP^{\alpha}(V_{\mathrm{ext}} + V_{\mathrm{bi}}), \tag{S6}$$

with the exponent α defining the current dependence on P. K is a proportionality constant and V_{bi} is a potentially existing built-in voltage. We chose this *ansatz* of a product of irradiance and voltage, as our experimental findings indicate that the two variables are indeed independent of each other. The associated quasi-Fermi-levels are sketched in Fig. S2 for the operation conditions discussed in the following.

In addition, thermally excited charge carriers can overcome the interface barrier and thus contribute to the current. The formation and height of this barrier, which is usually referred to as a Schottky barrier Φ_{B} [9,10], will not be discussed here. There are a number of models and descriptions in literature that deal with it[11–13]. However, when applying an external voltage, the charges in the semiconductor (or QDs) will be out of thermal equilibrium, which can be described by different quasi Fermi-levels for electrons and holes[14,15]. Assuming an n-doped semiconductor, this will primarily lead to a reduced electron density in the conduction band of the semiconductor in relation to the adjacent metal electrode. For a zero bias Schottky barrier height of $\Phi_{\mathrm{B},0}$ we assume for an applied bias V_{ext} a potential difference $\Phi_{\mathrm{B},0} + (1-\beta)e\,|V_{\mathrm{ext}}|$ between the conduction band and the quasi Fermi-level of the electrons $E_{\mathrm{F,n}}$ and a potential difference $\Phi_{\mathrm{B}} = \Phi_{\mathrm{B},0} - \beta e\,|V_{\mathrm{ext}}|$ between the conduction band and the Fermi-level E_{F} of the metal electrode. This means we consider a reduction of the Schottky barrier height by a fraction β of the applied external voltage V_{ext}, which leads to an occupation difference Δn in the Boltzmann approximation to the Fermi-Dirac function of

$$\Delta n = \exp\left(-\frac{\Phi_{\mathrm{B},0} - \beta e\,|V_{\mathrm{ext}}|}{k_{\mathrm{B}}T}\right) - \exp\left(-\frac{\Phi_{\mathrm{B},0} + (1-\beta)e\,|V_{\mathrm{ext}}|}{k_{\mathrm{B}}T}\right), \tag{S7}$$

with the elementary charge e, the Boltzmann constant k_{B} and the temperature T [16]. Multiplying eq. S7 with a diffusion constant C' and considering the sign of the bias voltage $s := \mathrm{sign}(V_{\mathrm{ext}})$ gives the resulting current I_{th} across the barrier as

$$I_{\mathrm{th}} = sC' \exp\left(-\frac{\Phi_{\mathrm{B},0}}{k_{\mathrm{B}}T}\right) \exp\left(-\frac{e\,(1-\beta_s)\,|V_{\mathrm{ext}}|}{k_{\mathrm{B}}T}\right) \left(\exp\left(\frac{e\,|V_{\mathrm{ext}}|}{k_{\mathrm{B}}T}\right) - 1\right), \tag{S8}$$

where the factor β has been equipped with an index s to take into account a possible asymmetry in the system due to different electrode materials and geometries. Finally, we combine the diffusion constant C' and the voltage-independent factor to the new constant C and define the ideality factor n_s by $1-\beta_s =: 1/n_s$, in accordance with the usual nomencla-

ture [5,16]. We thus model the diffusion current across the interface barriers as

$$I_{\mathrm{th}} = sC \exp\left(-\frac{e\,|V_{\mathrm{ext}}|}{n_s k_{\mathrm{B}} T}\right)\left(\exp\left(\frac{e\,|V_{\mathrm{ext}}|}{k_{\mathrm{B}} T}\right) - 1\right), \tag{S9}$$

which coincides with the description for thermionic emission over a single Schottky barrier that is biased in blocking direction. While this description has some limitations for large bias voltages, the resulting exponential form also explains other mechanisms described by Rhoderick and Williams [16], so we assume validity over a fairly large voltage range. The full model for the total current I is then given by the sum of eq. S6 and eq. S9 as

$$I = KP^{\alpha}(V_{\mathrm{ext}} + V_{\mathrm{bi}}) + sC \exp\left(-\frac{e\,|V_{\mathrm{ext}}|}{n_s k_{\mathrm{B}} T}\right)\left(\exp\left(\frac{e\,|V_{\mathrm{ext}}|}{k_{\mathrm{B}} T}\right) - 1\right). \tag{S10}$$

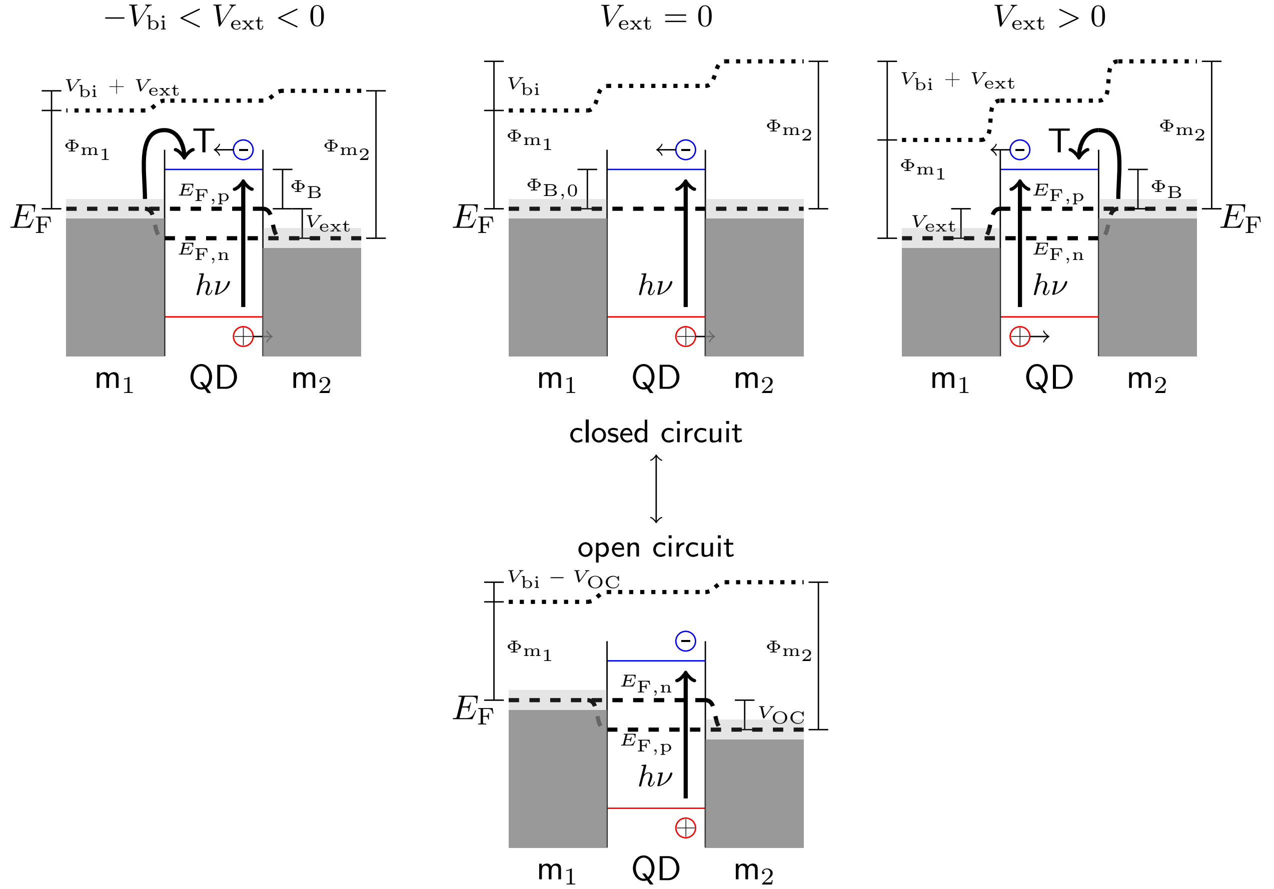

Fig. S2 Sketch of the quasi Fermi-levels (dashed lines) of electrons ($E_{\mathrm{F,n}}$) and holes ($E_{\mathrm{F,p}}$) and the vacuum levels (dotted lines) in a QD film between two metal electrodes (m_1, m_2) under various operation conditions. In the model, the QD film is assumed to be two-dimensional, therefore the horizontal lines shown in the QD area are to be understood as points. For electrode materials with different work functions (Φ_{m_1}, Φ_{m_2}) we expect in thermal equilibrium ($E_{\mathrm{F,n}} = E_{\mathrm{F,p}} = E_{\mathrm{F}}$) a built-in voltage V_{bi} across the junction. Illumination ($h\nu$) under open circuit conditions will generate excited charges which are separated by the built-in voltage and generate a non-zero open circuit voltage (V_{OC}). For a closed circuit, current flows and leads the system back towards thermal equilibrium. When applying an additional external voltage V_{ext} to the closed circuit, the system will again be out of thermal equilibrium, which drives an additional diffusion current of thermally excited (T) electrons across the Schottky barrier Φ_{B}. In our model we assume that the Schottky barrier height depends linearly on the applied external voltage with a barrier height $\Phi_{\mathrm{B},0}$ at $V_{\mathrm{ext}} = 0$.

We note that for thermionic emission over a Schottky barrier the diffusion constant C' can be expressed in terms of the effective Richardson constant A^* and the contact area F by [14]

$$C' = FA^*T^2\,, \tag{S11}$$

where A^* is related to the effective electron mass m^* and Planck's constant h via [17]

$$A^* = \frac{4\pi e m^* k_\mathrm{B}^2}{h^3}\,. \tag{S12}$$

For our experiment, we set the effective electron mass to $m^* = (0.095 \pm 0.010)$ times the electron mass m_0, averaged from literature values of $m^* = 0.085\,m_0$ for PbS QDs [18] and $m^* = 0.104\,m_0$ for $\mathrm{MAPbI_3}$ [19]. The Schottky barrier height $\Phi_{\mathrm{B},0}$ can therefore be estimated from the constant C, as

$$C = FA^*T^2 \exp\left(-\frac{\Phi_{\mathrm{B},0}}{k_\mathrm{B}T}\right)\,. \tag{S13}$$

As discussed in the main text, for the PbS/$\mathrm{MAPbI_3}$ QDs monolayer between PtIr and ITO electrodes we find values of $V_\mathrm{bi} = -0.70 \pm 0.02\,\mathrm{V}$, $n_+ = 1.026 \pm 0.003$, $n_- = 1.034 \pm 0.006$ and $C = 80 \pm 5\,\mathrm{fA}$.

We note that Arya et al.[20] proposed a physical model for colloidal QD junctions considering the carrier transport mechanisms in QDs. By including also quantum mechanical tunneling they derived the fundamental relationship

$$n_s = \frac{3e^2 h E_\mathrm{eq} V_\mathrm{bi}}{16\pi k_\mathrm{B} T \sqrt{2m^*}\,\Phi_{\mathrm{B},0}^{3/2}} \tag{S14}$$

between the built-in voltage V_bi, the ideality factor n_s and the interface barrier $\Phi_{\mathrm{B},0}$. The equilibrium electric field E_eq strength is implicitly given by[20]

$$\frac{\Phi_{\mathrm{B},0}}{k_\mathrm{B}T} - \frac{8\pi\sqrt{2m^*}}{3heE_\mathrm{eq}}\Phi_{\mathrm{B},0}^{3/2} = \ln\left(\frac{eE_\mathrm{eq}d}{k_\mathrm{B}T}\right), \tag{S15}$$

for the QD diameter d. This model allows us to estimate the interface barrier as $\Phi_{\mathrm{B},0} = 0.38 \pm 0.01$ eV, whereby a contact area of 10 - 30 nm^2, which corresponds to 1 - 3 QDs, can be concluded from eq. S13.

S4 pcAFM on PbS QDs ligand-exchanged with SCN

Corresponding to Fig. 4 from the main text, a similar series of measurements on a 10 nm thick PbS/SCN layer is shown in Fig. S3. The PbS QDs ligand-exchanged with SCN show a lower photoconductivity than the perovskite-capped QDs. However, they withstand higher light intensities, which is why the 60× objective was used. Consistently for all applied bias voltages, we find the irradiance dependence of the photocurrent to follow a power law with an exponent of $\alpha = 0.35 \pm 0.03$. From the associated I/V curve, an Ohmic contribution of 0.5 pA/V (as discussed in the context of the PbS/$MAPbI_3$ monolayer in the main text) is found for an applied light irradiance of 100 W/cm^2.

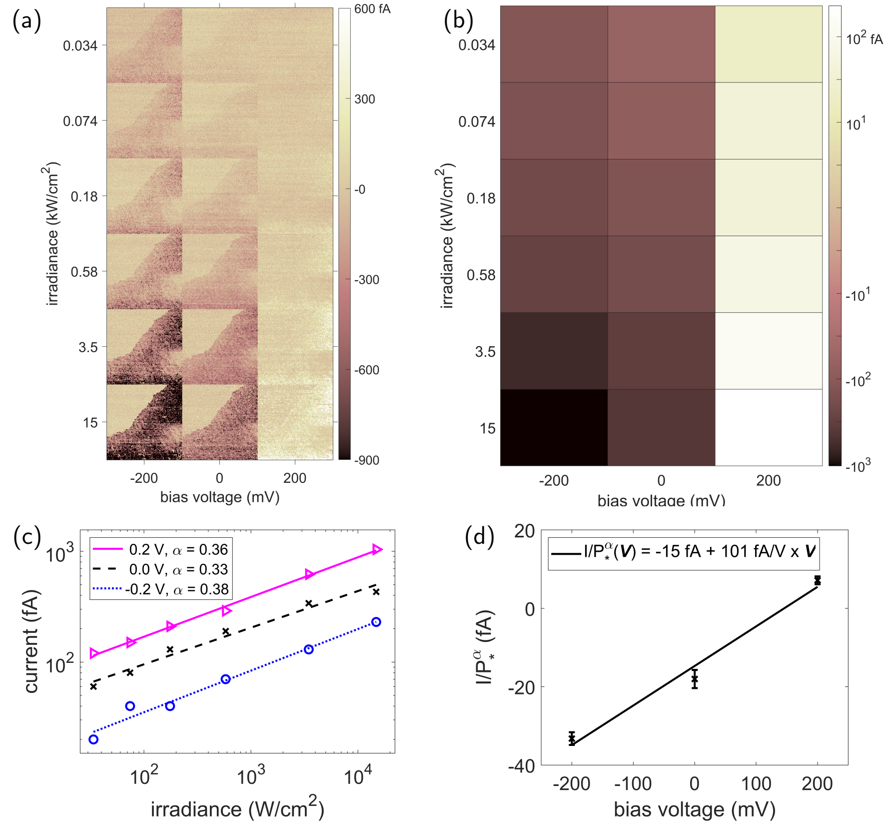

Fig. S3 Peak force tapping pcAFM measurements on a 10±2 nm thick PbS/SCN QD layer on ITO. (a) Current maps for bias values of -200 - 200 mV (rows) and irradiances of 0 - 15 kW/cm^2 (columns), delivered through the 60× objective. The scan areas measure $10 \times 10\,\mu m^2$. (b) Heat map of the averaged current values over the QD-covered areas of panel (a). (c) Measured irradiance-dependent currents (symbols) and power law fits (lines) for each bias voltage. (d) Fit of Ohm's law to the voltage-dependent current scaled by the derived power law with $\alpha = 0.35$, $P_* = P/(1\,W/cm^2)$, P being the corresponding irradiance.

S5 cAFM on gold structures

For reference, we probed bare lithographed gold nanostructures by cAFM. Fig. S4 shows exemplarily topography and current map, respectively, of a gold nanodisk dimer. As observed for all gold structures investigated, a conductive connection between the AFM tip and gold is only established around structure edges or prominent roughness features. There, increased interaction forces are expected between tip and sample due to the finite AFM feedback response time. The exemplary I/V curve acquired at a position of stable conductive contact shows Ohmic behaviour. With a resistance of about 20 MΩ, amplifier saturation was reached for a bias of ±200 mV. This Ohmic behaviour is observed in any case once a conducting connection is established on the gold surface. We note that similar observations are made on the bare ITO substrate, where contact is however only established on rare protruding grains on the otherwise very flat surface. Additional laser illumination as in the pcAFM measurements did not have any influence on these observations.

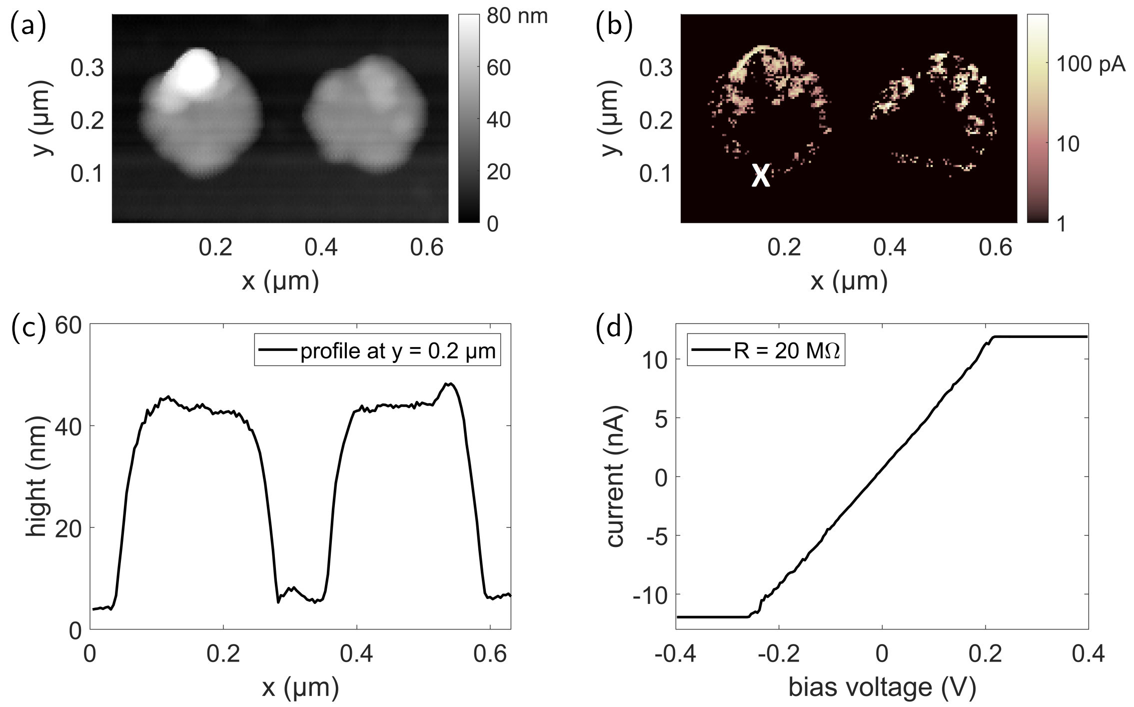

Fig. S4 Peak force tapping cAFM imaging of a dimer of gold nanodisks with 200 nm diameter for 30 mV bias voltage, measured in a nitrogen cell. (a) Topography, (b) current map, (c) height profile extracted from (a) at a y-axis position of 0.2 μm, (d) I/V curve acquired at the position marked "X" in (b) with established contact between gold and tip, the corresponding Ohmic resistance is about 20 MΩ at a contact force of 3 nN.

References

1 O. Svelto and D. C. Hanna, *Principles of lasers*, Plenum Press, New York, 3rd edn, 1989.

2 M. Drndic, M. Vitasovic, N. Morgan, M. Kastner and M. Bawendi, *J. Appl. Phys.*, 2002, **92**, 7498–7503.

3 Y. Zhang, K. Miszta, S. Kudera, L. Manna, E. Di Fabrizio and R. Krahne, *Nanoscale*, 2011, **3**, 2964–2970.

4 J. Chiquito, C. Amorim, O. Berengue, L. Araujo, E. Bernardo and E. Leite, *J. Phys. Condens. Matter*, 2012, **24**, 225303.

5 Y. Fan, Y. Zhou, X. Wang, H. Tan, Y. Rong and J. Warner, *Adv. Opt. Mater.*, 2016, **4**, 1573–1581.

6 A. Grillo and A. Di Bartolomeo, *Adv. Electron. Mater.*, 2020, **7**, 2000979.

7 A. Rose, *Concepts in photoconductivity and allied problems*, Interscience Publishers, New York, 1963.

8 D. Grimaldi, E. Kelderer, D. N. Dirin, M. Kovalenko, V, A. Hohenau, H. Ditlbacher and J. R. Krenn, *Nanoscale Adv.*, 2022, **4**, 3566–3572.

9 W. Schottky, *Naturwissenschaften*, 1938, **26**, 843.

10 H. Hasegawa, *Jpn. J. Appl. Phys.*, 1999, **38**, 1098.

11 W. Mönch, *J. Vac. Sci. Technol. B*, 1988, **6**, 1270–1276.

12 C. Mead, *Solid State Electron.*, 1966, **9**, 1023–1033.

13 A. M. Cowley and S. M. Sze, *J. Appl. Phys.*, 1965, **36**, 3212–3220.

14 S. M. Sze and M. K. Lee, *Semiconductor Devices: Physics and Technology*, John Wiley & Sons, New York, 3rd edn, 2012.

15 C. Kagan, E. Lifshitz, E. Sargent and D. Talapin, *Science*, 2016, **353**, aac5523–aac5523.

16 E. Rhoderick and R. Williams, *Metal-Semiconductor Contacts*, Oxford University Press, Oxford, 2rd edn, 1988.

17 H. Wong, J. Zhang and J. Liu, *Nanomaterials*, 2024, **14**, 386.

18 K. Nanda, F. Kruis, H. Fissan and S. Behera, *J. Appl. Phys.*, 2004, **95**, 5035–5041.

19 K. Gałkowski, M. Anatolie, A. Miyata, P. Plochocka, O. Portugall, G. Eperon, J. Wang, T. Stergiopoulos, S. Stranks, H. Snaith and R. Nicholas, *Energy Environ. Sci.*, 2016, **9**, 962–970.

20 S. Arya, Y. Jiang, B. Jung, Y. Tang, T.-N. Ng, S. Oh, K. Nomura and Y.-H. Lo, *Nano Lett.*, 2023, **23**, 9943–9952.